



Correspondence

Congenital lactic acidosis, cerebral cysts and pulmonary hypertension in an infant with FOXRED1 related complex 1 deficiency



A B S T R A C T

Mitochondrial complex I is encoded by 38 nuclear-encoded and 7 mitochondrial-encoded genes. *FOXRED1* is one of the 13 additional nuclear genes known as assembly factors. So far, four patients have been described with complex I deficiency caused by autosomal recessive mutations in *FOXRED1*.

Here, we report the fifth patient with *FOXRED1* related complex 1 deficiency presenting with prenatal onset of bilateral periventricular cysts, congenital lactic acidosis, and persistent life-limiting pulmonary hypertension. Whole exome sequencing identified a compound heterozygosity for a known pathogenic variant (c.612_615dupAGTG; p.A206SfsX15) (paternal) and a likely pathogenic variant (c.874G > A; p.Gly292Arg) (maternal). Deficiency of complex I was demonstrated by the absence of complex I on Blue Native Gel Electrophoresis and by a significantly reduced complex I enzyme activity in the patient's fibroblasts.

Compared with the previous known *FOXRED1* cases, unique clinical features observed in our patient include bilateral periventricular cysts and severe pulmonary hypertension. Whole exome sequencing was instrumental in recognizing the underlying gene defect in this patient.

1. Introduction/background

The mitochondrial complex I (NADH: ubiquinone oxidoreductase) is the first and largest complex of the respiratory chain, which is composed of a total of 45 subunits including 7 mitochondrial and 38 nuclear encoded subunits. In addition to structural components, a number of proteins/putative assembly factors are involved in the assembly, stability and regulation of the 980 kDa complex I holoenzyme, namely one flavin mononucleotide and 8 iron-sulfur clusters. Currently, 13 of the genes encoding factors composing mitochondrial complex I have been linked to human disease (*NDUFA1*, *NDUFA2*, *NDUFA3*, *NDUFA4*, *C20ORF7*, *C8ORF38*, *NUBPLACAD9*), in addition to the FAD-dependent oxidoreductase domain-containing protein 1 (*FOXRED1*).

FOXRED1 encodes a 486-amino acid FAD-dependent oxidoreductase domain involved in mid-late stage of complex I assembly. Recently, *FOXRED1* mutations have been recognized as a cause of complex I deficiency. In the absence of a functional *FOXRED1* protein, mtDNA-encoded complex I subunits are still translated and transiently assembled into a late stage ~815 kDa intermediate, however, instead of transitioning further to the mature complex I, the intermediate breaks down to an ~475 kDa complex. A similar mechanism has been observed in cells lacking the *NDUFA9* subunit [1,5].

Mutations in this gene are rare as only 4 patients have been described so far in the literature [1–3]. The clinical presentation of defects in *FOXRED1* varies from infantile onset encephalomyopathy and Leigh syndrome [2] to epileptic encephalopathy with severe psychomotor retardation [3]. Here we describe a fifth patient with *FOXRED1* related complex 1 deficiency, presenting with intrauterine cerebral periventricular cysts, neonatal lactic acidosis, and pulmonary hypertension.

2. Case report

A female infant, the 1st product of conception of a non-consanguineous marriage, was admitted to the neonatal intensive care unit (NICU) at 23 h of life because of severe lactic acidosis. First evidence of intrauterine growth retardation (IUGR) was noted at 28 weeks of

gestation. Follow-up ultrasound at 35 weeks confirmed oligohydramnios, severe symmetrical IUGR (head circumference and abdominal circumference below 1st centile and femur length at 7th centile), and cerebral periventricular cysts with mild / moderate ventriculomegaly. The baby was delivered after induction of labor at 37 weeks with APGAR scores 9 and 9, a birth weight of 2010 g (3rd %ile), a length of 43.5 cm (3rd %ile), and a head circumference of 30 cm (3rd %ile). Blood glucose checks during the first 20 h of life were borderline low (2.2–2.8 mmol/L) but rapidly improved on milk supplementation.

At 22 h, she developed hypothermia (35.1–36.0° C), tachypnea with desaturations (SPO₂ 81–89%), severe metabolic acidosis (pH 6.9, bicarbonate 3 mmol/L), and an arterial blood lactate of 20 mmol/L; blood cultures were negative. Treatment with biotin 20 mg (q12 hrs), levocarnitine 100 mg (q12 hrs), thiamine 200 mg (q12 hrs), riboflavin 100 mg (q6 hrs), coenzyme Q10 90 mg (q6 hrs), and alpha lipoic acid 25 mg (q12 hrs) did not improve blood lactic acid levels. After 4 dosages of dichloroacetate (DCA) (25 mg/kg/day q12 hrs enterally), her blood lactate levels decreased from 18.3 mmol/L to 3.3 mmol/L. Blood lactate levels were maintained at 1.0–3.3 mmol/L during the 20 day course of treatment and remained within this range for 5 weeks (37 days) after discontinuation of DCA.

On the second day of life, she developed hypotension and generalized seizures. A continuous amplitude integrated EEG showed a pattern of burst suppression. Hypotension and seizures improved on treatment with Phenobarbital and Nitric oxide.

An echocardiogram performed at 34 h showed pulmonary hypertension with a dilated right ventricle and atrium, a patent ductus arteriosus and foramen ovale, both with right to left shunts. Due to progressive respiratory decompensation, she was placed on mechanical ventilation for 3 weeks and treated with inhaled nitric oxide (iNO) and vasopressors. She remained on oxygen supply via optiflow nasal prongs for persistent bradycardias, desaturations, and echocardiographic findings of supra-systemic pulmonary hypertension. Sildenafil was started to a maximum dose of 8 mg/kg/day, while iNO was gradually weaned off.

<https://doi.org/10.1016/j.ymgmr.2019.100472>

Received 4 April 2019; Received in revised form 18 April 2019; Accepted 18 April 2019

Available online 30 April 2019

2214-4269/© 2019 Published by Elsevier Inc. This is an open access article under the CC BY-NC-ND license

(<http://creativecommons.org/licenses/by-nc-nd/4.0/>).

On day 59, the baby experienced a second episode of lactic acidosis (pH 7.04, pCO₂ 32 mmHg, HCO₃ 8 mmol/L, lactate 19 mmol/L), which normalized upon reintroduction of DCA treatment.

On day 68 (2.5 months of age), a repeat echocardiogram showed evidence of persistent severe pulmonary hypertension (estimated right ventricular pressure of 110 mmHg based on tricuspid jet measurements with dilatation of the right ventricle and right atrium) with compensated bi-ventricular function and a closed ductus arteriosus.

She remained on CPAP and passed away at 3 months of age.

3. Results of investigations

3.1. Brain imaging

The initial postnatal (< 24 h from birth) head ultrasound revealed large periventricular cysts with smaller cysts in the internal capsule and basal ganglia. The periventricular cysts are similar to those seen in Holocarboxylase (multiple carboxylase) deficiency. Magnetic Resonance Imaging was performed on day 13 of life showing large periventricular cysts, edematous white matter, delayed myelination, thin and undersulcated cortex particularly anteriorly. Proton magnetic resonance spectroscopy (MRS) showed a markedly elevated cerebral lactate (Fig. 1).

3.2. Metabolic work up

Organic acids showed marked lactic aciduria, marked ketonuria and large excretion of tyrosine metabolites typically seen with liver dysfunction or liver immaturity. Bloodspot acylcarnitine showed evidence of ketonemia in an otherwise unremarkable profile. Plasma amino acids showed increased alanine and proline consistent with a primary lactic

acidosis. Blood pyruvate was increased (0.315 mmol/L normal range 0.067–0.130 mmol/L) and the lactate to pyruvate ratio was elevated which was in line with the presence of a mitochondrial disorder.

3.3. Autopsy findings

Autopsy was limited to biopsies of lung and muscle. The lung biopsies showed marked pulmonary arterial hypertensive changes with medial hypertrophy, intimal hyperplasia, early intimal fibrosis, and narrowing of the lumina of small pulmonary arteries. There was focal disruption of the internal elastic lamina of the occasional small pulmonary artery with Masson-elastic stains. In addition, there was decreased alveolarization and thickened alveolar walls (Fig. 2). Quadriceps femoris muscle biopsy was normal by histology and with histochemical stains. Ultrastructurally, there were scattered large mitochondria with whorled cristae. Abundant glycogen was present in a subsarcolemmal and intermyofibrillar distribution.

3.4. Genetic testing

Whole Exome Sequencing (Trio) and whole mitochondrial genome sequencing and deletion testing was performed in DNA extracted from blood, and carried out by a commercial laboratory (GeneDx) according to previously described method [9,10]. The results revealed 2 variants in *FOXRED1*: [c.612_615dupAGTG (p.A206SfsX15)], classified as pathogenic, paternally inherited and [c.874G > A (p.Gly292Arg)], classified as likely pathogenic, maternally inherited (Figs. 3 and 4).

3.5. Biochemical characterization of Complex 1 deficiency

In order to validate the significance of the identified *FOXRED1*

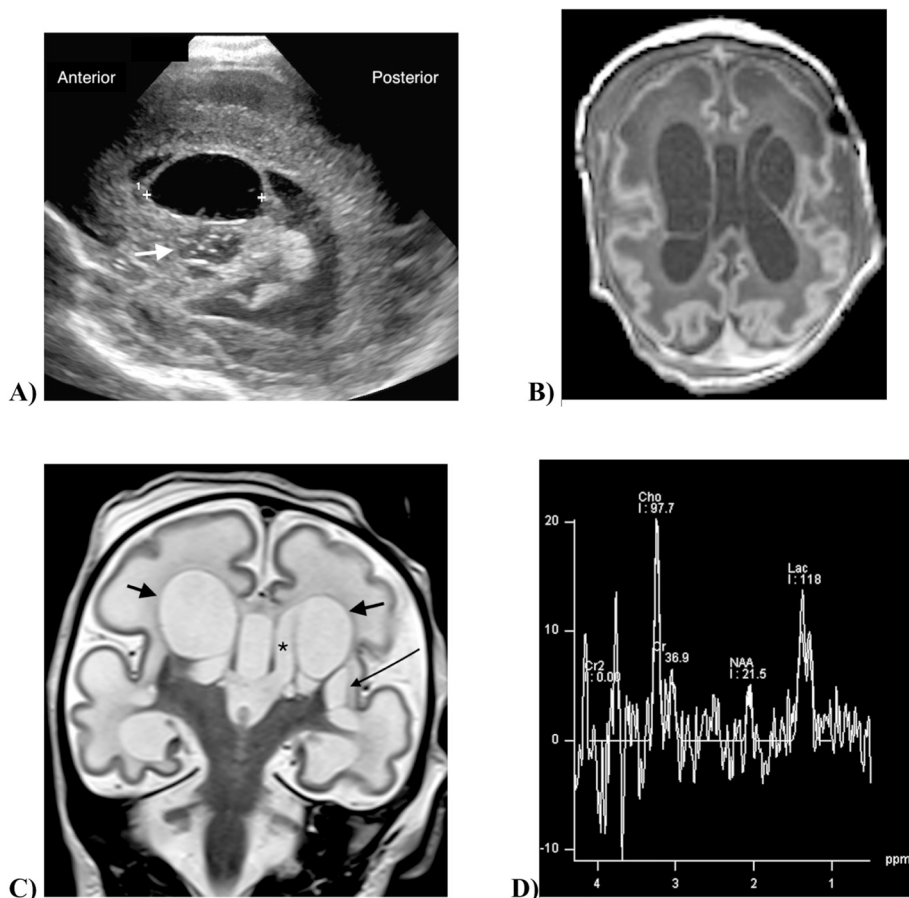


Fig. 1. Neuroimaging in an infant with *FOXRED1*-related complex 1 deficiency and cerebral cysts.

(A) Cranial ultrasound on the first day of life. Parasagittal image in the plane of the left lateral ventricle shows a large cyst (markers) invaginating into the lateral ventricle. Bubbly cystic change is seen in the basal ganglia inferior to the cyst (arrow). (B) Axial T1-weighted MR scan at 13 days of age shows large bilateral periventricular cysts. There is diffusely reduced gyral complexity with shallow sulci, most marked in the frontal lobes. The periventricular and subcortical white matter is diffusely T1-hypointense.

(C) Coronal T2-weighted MR scan shows bilateral periventricular cysts (short arrows) adjacent to the lateral ventricles (asterisk). Small cysts are present in the left basal ganglia (long arrow). The sylvian fissures and cerebral cortex are simple, and there is diffuse T2-hyperintensity of the white matter including the corpus callosum.

(D) Single voxel MR spectroscopy at TE288 in the right basal ganglia shows increased brain lactate with a lactate doublet at 1.3 ppm, and markedly diminished NAA (*N*-acetyl aspartic acid).

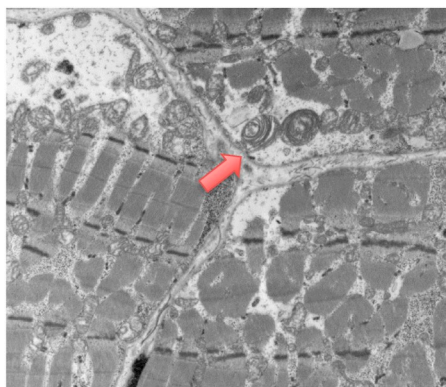
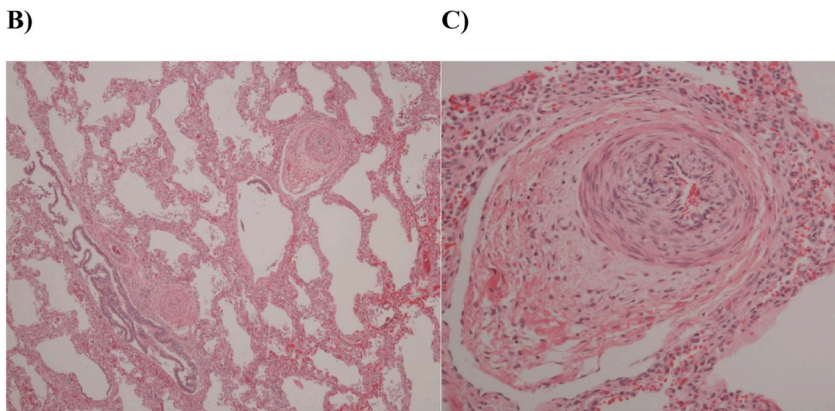


Fig. 2. Autopsy findings in a female infant with *FOXRED1* related complex 1 deficiency presenting with neonatal lactic acidosis and cerebral cysts and pulmonary hypertension leading to exitus lethalis on 2.5 month of age. A) Electron microscopy of the quadriceps femoris shows abnormal mitochondria with increased size and whorled cristae (arrow); Light microscopy of the Pulmonary artery with Hematoxylin and Eosin stain shows B) (mag x50) Pulmonary arterial hypertensive changes with medial hypertrophy and luminal narrowing in small arteries. Alveolar walls are thickened and there is alveolar simplification; C) (mag x200) Pulmonary arterial hypertensive changes in small Pulmonary artery with medial hypertrophy, intimal hyperplasia and narrowing of the lumen.



variants, analysis of mitochondrial oxidative phosphorylation (OXPHOS) complexes was performed in the patient's fibroblasts obtained from a skin biopsy taken within 12 hours post-mortem). Tests were done in duplicates according to established methods by a clinical diagnostic lab (CHU Sainte-Justine Biochemical Genetics Diagnostic Laboratory, Montreal). The enzymatic activity of complex I (expressed as complex I / complex II ratio) was 18% of mean normal activity, confirming complex I deficiency. Complex II normalized to citrate synthase activity was within the normal range (Table 1).

showed a significant decrease in CI/CII assembly level in patient's fibroblast (8% of mean normal control value) (Fig. 5B). The CIV/CII assembly level was within normal range although the gel showed somewhat different band migration for CIV, which may be suggestive of a supercomplex. It is possible that this supercomplex is secondary to the complex I assembly defect. Blue native gel was done in duplicate and the patient's sample was tested in duplicate on each gel. See Fig. 5A.

Blue-Native Polyacrylamide Gel Electrophoresis (BN-PAGE) analysis

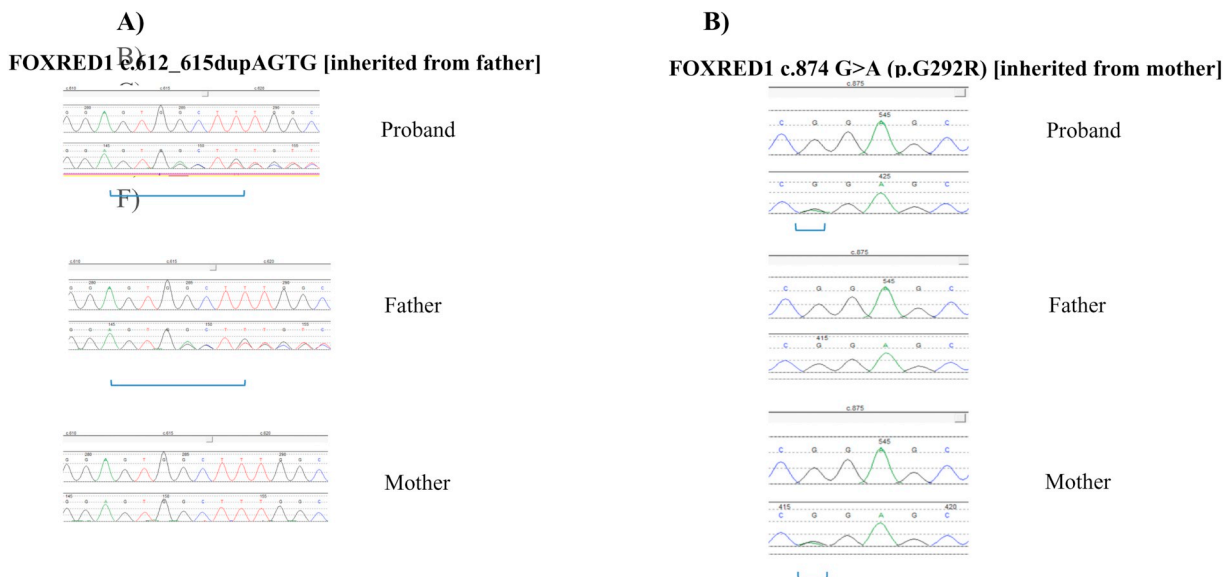


Fig. 3. *FOXRED1* sequencing chromatogram showing the affected proband's mutations inherited from father A): c.612_615dupAGTG, and mother B): c.874G > A (compound heterozygous).

Table 1

Respiratory chain complex activities in a patient with compound heterozygous variants in *FOXRED1* presenting congenital lactic acidosis, cerebral cysts and pulmonary hypertension.

| Ratio | Normalized enzymatic activities | |
|---------------|---------------------------------|--|
| | Patient | Reference values range (median) N = 12 |
| CI/CII | 0.13 (18%) | 0.15–1.13 (0.70) |
| CII/CS | 0.54 (135%) | 0.32–0.50 (0.40) |
| CIII/CII | 2.41(88%) | 1.94–3.25 (2.75) |
| CII + CIII/CS | 0.37 (112%) | 0.29–0.47 (0.33) |
| CIV/CII | 3.18 (82%) | 2.80–4.39 (3.88) |
| CV/CII | 0.90 (63%) | 1.14–1.88 (1.43) |

CS = citrate synthase; CI = complex I, CII = Complex II, CIII=Complex III CIV = Complex IV, CV=Complex V CII + CII = succinyl cytochrome *c* oxydoreductase (combined activity of CII and CIII) for indirect measure of Coenzyme Q. % of patient value refers to median reference value.

complex I deficiency, as in our patient, the pathomechanism underlying PH is not fully understood. One explanation might be that impaired oxidative phosphorylation predisposes pulmonary arterial cells to switch to glycolysis and thereby develop hyperproliferation and resistance to apoptosis as seen in primary PH.

The severe lactic acidosis in our patient was responsive to DCA. DCA shifts glycolysis-derived pyruvate towards the Krebs cycle and oxidative phosphorylation through inhibition of pyruvate dehydrogenase kinase and consecutive enhancement of pyruvate dehydrogenase activity. Although this mechanism counteracts the Wardenburg effect in PH, administration of DCA did not prevent life-limiting PH in our patient. The limited clinical benefit of DCA treatment in our patient is in line with results from two randomized controlled trials showing effectiveness of DCA in reducing blood lactate levels but ineffectiveness in improving clinical outcomes [7] [9]. A separate trial of DCA in children with MELAS showed that long term administration of DCA led to nerve toxicity without any clinical benefit [8].

The four patients described so far with *FOXRED1* deficiency harbor 6 different *FOXRED1* variants, including 4 missense, 1 nonsense and 1 frameshift variant (Table 2). The duplication changes in the known frameshift variant (c.612_615dupAGTG) changes alanine 206 to a

serine residue, causes a frameshift, and creates a premature stop codon at position 15 of the new reading frame. This pathogenic variant is predicted to cause a loss of normal protein function either through protein truncation or nonsense-mediated mRNA decay [5].

Our patient carried this frameshift variant on the paternal *FOXRED1* allele. The Gly292Arg variant on the maternal allele has not been described in a diseased human before. The variant has been reported in heterozygosity in 3 of 244,118 adults in the gnomAD database (Ref: <http://gnomad.broadinstitute.org/>) but has not been observed at a significant frequency in large population cohorts. Gly292Arg is conserved in insects and worms. The non-conservative amino acid substitution is likely to impact secondary protein structure as these residues differ in polarity, charge, size and/or other properties. In silico analyses predict this variant is probably damaging to the protein structure and function.

Validation studies including the overexpression of *FOXRED1* mutations and wildtype rescue studies were completed in all previous cases. We have not been able to perform overexpression and wildtype rescue studies in our patient, however biochemical phenotyping in fibroblasts including Blue Native Gel and OXPHOS complex activities showed a deficiency of complex I supporting the pathogenicity of the likely pathogenic variant Gly292Arg. We will actively seek in Gene Matcher for cases with similar clinical presentation and Gly292Arg mutation for further clarification of pathogenicity of Gly292Arg variant.

Overall, this case report expands the clinical and molecular genetic spectrum of *FOXRED1* deficiency and associated complex I deficiency. We were able to demonstrate the functional impact of the compound heterozygous variants in our patient, which severely impacted complex I assembly and activity thus providing a basis for genetic counselling. Our report further highlights the key role of mitochondria in pediatric PH.

Consent

The parents provided written consent for the publication of this case report and accompanying images and edited the final 2 drafts of the manuscript for accuracy. We are grateful for their contributions. The informed consent was reviewed and approved by the British Columbia Provincial Health Services Authority, Ethics Service.

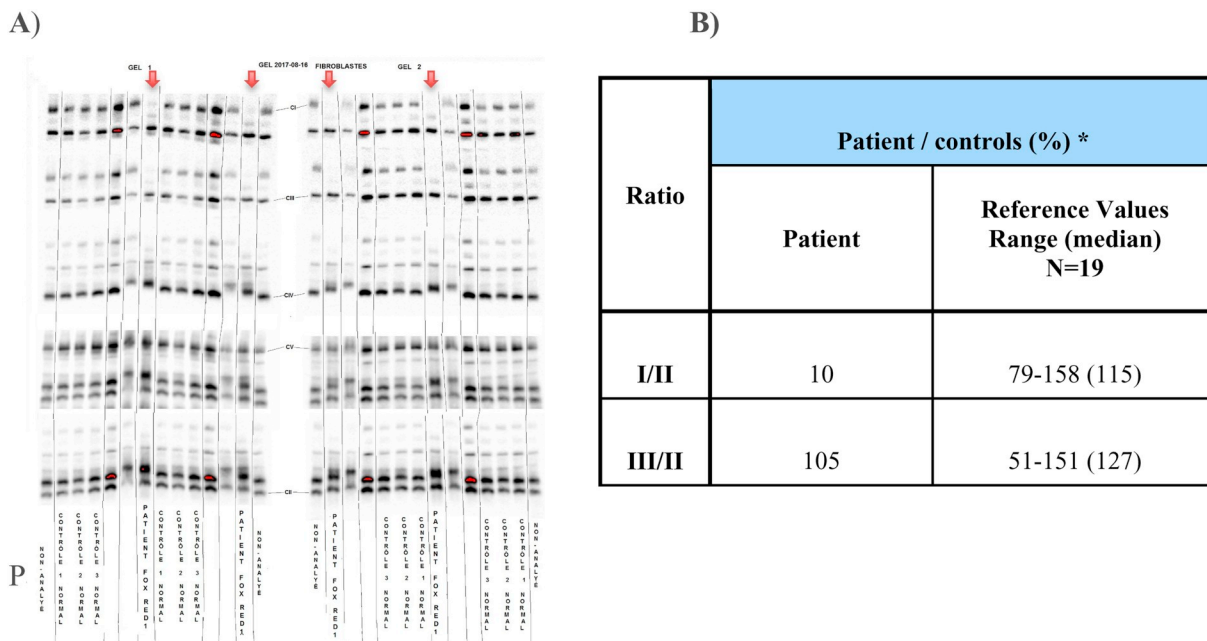


Fig. 5. Mitochondrial respiratory chain analysis by Blue Native-PAGE: (A) Blue-Native PAGE gel showing complex I deficiency in the patient (patient run in duplicate on two different gels along with normal controls). (B) Density measurements of the patient bands compared to normal controls.

Table 2
Genotype and phenotypic features observed in 5 patients described so far with FOXRED1 deficiency.

| Case # | Genetic mutation | Zygosity | Clinical diagnosis | Metabolic/biochemical findings | Neurological findings | MRI features |
|-------------------------|---|-----------------------|---|--|---|---|
| Case 1 [2] | p.R352W/(p.Arg352Trp) c.1054C > T missense variant | Homozygous | Leigh syndrome | Elevated plasma lactate Decreased level of C I | Severe truncal hypotonia/ Mitochondrial encephalopathy | Delayed myelination, ventricular dilatation and abnormal signal in thalami and basal ganglia |
| Case 2 [1] | p.N430S/(p.Asn430Ser) c.1289A > G missense variant p.Q232X/(p.Gln232Ter) c.694C > T nonsense variant p.V421M/(p.Val421Met) c.1308G > A missense variant | Compound heterozygous | Leigh syndrome | Hypoglycemia Lactic acidosis Decreased level of C I Complex I and II deficiency | Hypotonia Athetoid movements | Decreased attenuation in the putamen bilaterally and significant cerebellar atrophy |
| Case 3 [3] | p.V421M/(p.Val421Met) c.1308G > A missense variant | Homozygous | Severe encephalopathy | | Epilepsy Severe psychomotor retardation | Delayed myelination, ventricular dilatation and abnormal signal in the thalami and basal ganglia |
| Case 4 [5] | c.406C > T; p.R136W missense variant c.612_615dupAGTG; p-Ala206SerfsX15 frameshift variant | Compound heterozygous | (Clinical diagnosis not defined) | Complex I activity < 25 | N/A | N/A |
| Case 5 (our index case) | p. Ala206SerfsX15 frameshift variant p. Gly292Arg c.874G > A missense variant | Compound heterozygous | Neonatal lactic acidosis, cerebral cysts and Pulmonary Hypertension | Decreased activity of complex I (Decreased C I and II) | Mild hypertonia, wrist and ankle contracture. | Diffusely abnormal brain with large periventricular cysts, edematous white matter, delayed myelination, thin and undersulcated cortex particularly anteriorly |

Contributions

All authors critically revised the manuscript and approved the version to be published. Images were obtained and reviewed at BC Children's Hospital. GeneDx performed the whole exome sequencing analysis and CHU Sainte-Justine Biochemical Genetics Laboratory conducted the functional complementation studies.

References

- [1] L. Formosa, M. Mimaki, A. Frazier, et al., Characterization of mitochondrial FOXRED1 in the assembly of respiratory chain complex I, *Hum. Mol. Genet.* 24 (10) (2015) 2952–2965, <https://doi.org/10.1093/hmg/ddv058>.
- [2] E. Fassone, A. Duncan, J. Taanman, et al., FOXRED1, encoding an FAD-dependent oxidoreductase complex-I-specific molecular chaperone, is mutated in infantile-onset mitochondrial encephalopathy, *Hum. Mol. Genet.* 19 (24) (2010) 4837–4847, <https://doi.org/10.1093/hmg/ddq414>.
- [3] O. Zurita Rendón, H. Antonicka, R. Horvath, E. Shoubridge, A mutation in the flavin adenine dinucleotide-dependent oxidoreductase FOXRED1 results in cell-type-specific assembly defects in oxidative phosphorylation complexes I and II, *Mol. Cell. Biol.* 36 (16) (2016) 2132–2140, <https://doi.org/10.1128/mcb.00066-16>.
- [4] R. Rafikov, X. Sun, O. Rafikova, et al., Complex I dysfunction underlies the glycolytic switch in pulmonary hypertensive smooth muscle cells, *Redox Biol.* 6 (2015) 278–286, <https://doi.org/10.1016/j.redox.2015.07.016>.
- [5] T. Haack, F. Madignier, M. Herzer, et al., Mutation screening of 75 candidate genes in 152 complex I deficiency cases identifies pathogenic variants in 16 genes includingNDUFB9, *J. Med. Genet.* 49 (2) (2011) 83–89, <https://doi.org/10.1136/jmedgenet-2011-100577>.
- [6] A. Barclay, G. Sholler, J. Christodolou, et al., Pulmonary hypertension—a new manifestation of mitochondrial disease, *J. Inher. Metab. Dis.* 28 (6) (2005) 1081–1089, <https://doi.org/10.1007/s10545-005-4484-x>.
- [7] U. Ahting, J. Mayr, A. Vanlander, et al., Clinical, biochemical, and genetic spectrum of seven patients with NFU1 deficiency, *Front. Genet.* 06 (2015), <https://doi.org/10.3389/fgene.2015.00123>.
- [8] A. Navarro-Sastre, F. Tort, O. Stehling, et al., A fatal mitochondrial disease is associated with defective NFU1 function in the maturation of a subset of mitochondrial Fe-S proteins, *Am. J. Hum. Genet.* 89 (5) (2011) 656–667, <https://doi.org/10.1016/j.ajhg.2011.10.005>.
- [9] K. Retterer, J. Juusola, M. Cho, et al., Clinical application of whole-exome sequencing across clinical indications, *Genet. Med.* 18 (7) (2015) 696–704, <https://doi.org/10.1038/gim.2015.148>.
- [10] N. Lake, B. Webb, D. Stroud, et al., Biallelic mutations in MRPS34 lead to instability of the small mitoribosomal subunit and Leigh syndrome, *Am. J. Hum. Genet.* 102 (4) (2018) 713, <https://doi.org/10.1016/j.ajhg.2018.03.015>.

Delia Apatan^{a,*}, Bojana Rakic^b, Catherine Brunel-Guitton^c, Glenda Henderson^d, Renkui Bai^e, Michael A. Sargent^f, Pascal M. Lavoie^g, Millan Patel^h, Sylvia Stockler-Ipsirogluⁱ

^a Division of Biochemical Diseases, Department of Pediatric, BC Children's Hospital, UBC, Room K3-206, 4480 Oak Street, Vancouver, BC V6H 3V4, Canada

^b BC Newborn Screening Program and Biochemical Genetics Lab, BC Children's Hospital and BC Women's Hospital & Health Centre, 2F16-4500 Oak Street, Vancouver, BC V6H 3N1, Canada

^c Department of Pediatrics, CHU Sainte-Justine, 3175, chemin Cote Sainte-Catherine, Montreal, QC H3T 1C5, Canada

^d Department of Pathology, BC Children's Hospital and BC Women's Hospital & Health Centre, 2H56-4500 Oak Street, Vancouver, BC V6H 3N1, Canada

^e GeneDx, 207 Perry Parkway, Gaithersburg, MD 20877, United States of America

^f Department of Radiology, BC Children's Hospital, University of British Columbia, Room 1L72, 4480 Oak Street, Vancouver, BC V6H 3V4, Canada

^g BC Children's Hospital Research Institute, Room A4-147, 4th floor Translational Research Building, 950 West 28th Avenue, Vancouver, BC

V5Z 4H4, Canada

^h Department of Medical Genetics, UBC, Room C234, 4500 Oak Street,
Vancouver, BC V6H 3N1, Canada

ⁱ Head Division of Biochemical Genetics, BC Children's Hospital, University
of British Columbia, Room K3-205, 4480 Oak Street, Vancouver, BC V6H
3V4, Canada

E-mail addresses: Delia.Apatean@cw.bc.ca (D. Apatean),
Bojana.Rakic@cw.bc.ca (B. Rakic),
catherine.brunel-guitton.hsj@ssss.gouv.qc.ca (C. Brunel-Guitton),
ghendson@cw.bc.ca (G. Hendson), RBai@genedx.com (R. Bai),
msargent@cw.bc.ca (M.A. Sargent), plavoie@cw.bc.ca (P.M. Lavoie),
mPatel@cw.bc.ca (M. Patel), stockler@cw.bc.ca (S. Stockler-Ipsiroglu).

* Corresponding author at: Division of Biochemical Genetics, Department of Pediatrics, BC Children's Hospital, University of British Columbia, Room K3-206, 4480 Oak Street, Vancouver BC V6H 3V4, Canada.